Maastricht University

Gene expression profiling in colon of mice exposed to food additive titanium dioxide (E171)

Citation for published version (APA):

Proquin, H., Jetten, M. J., Jonkhout, M. C. M., Garduno-Balderas, L. G., Briede, J. J., de Kok, T. M., Chirino, Y. I., & van Loveren, H. (2018). Gene expression profiling in colon of mice exposed to food additive titanium dioxide (E171). *Food and Chemical Toxicology*, *111*, 153-165. https://doi.org/10.1016/j.fct.2017.11.011

Document status and date:
Published: 01/01/2018

DOI:
10.1016/j.fct.2017.11.011

Document Version:
Publisher's PDF, also known as Version of record

Document license:
Taverne

Please check the document version of this publication:

• A submitted manuscript is the version of the article upon submission and before peer-review. There can be important differences between the submitted version and the official published version of record. People interested in the research are advised to contact the author for the final version of the publication, or visit the DOI to the publisher's website.
• The final author version and the galley proof are versions of the publication after peer review.
• The final published version features the final layout of the paper including the volume, issue and page numbers.

Link to publication

General rights
Copyright and moral rights for the publications made accessible in the public portal are retained by the authors and/or other copyright owners and it is a condition of accessing publications that users recognise and abide by the legal requirements associated with these rights.

• Users may download and print one copy of any publication from the public portal for the purpose of private study or research.
• You may not further distribute the material or use it for any profit-making activity or commercial gain
• You may freely distribute the URL identifying the publication in the public portal.

If the publication is distributed under the terms of Article 25fa of the Dutch Copyright Act, indicated by the “Taverne” license above, please follow below link for the End User Agreement:

www.umlib.nl/taverne-license

Take down policy
If you believe that this document breaches copyright please contact us at:

repository@maastrichtuniversity.nl

providing details and we will investigate your claim.

Download date: 19 Apr. 2024

Food and Chemical Toxicology 111 (2018) 153–165

Contents lists available at ScienceDirect

Food and Chemical Toxicology

journal homepage: www.elsevier.com/locate/foodchemtox

Gene expression profiling in colon of mice exposed to food additive titanium dioxide (E171)

Héloïse Proquin[a,*], Marlon J. Jetten[a], Marloes C.M. Jonkhout[a], Luis G. Garduño-Balderas[b], Jacob J. Briedé[a], Theo M. de Kok[a], Yolanda I. Chirino[b,c], Henk van Loveren[a]

[a] Department of Toxicogenomics, GROW Institute of Oncology and Developmental Biology, Maastricht University, The Netherlands
[b] Laboratorio de Carcinogénesis y Toxicología, Unidad de Biomedicina, FES-Iztacala, UNAM, Estado de México, Mexico
[c] IUF-Leibniz Research Institute for Environmental Medicine, Auf'm Hennekamp 50, 40225 DE Düsseldorf, Germany

ARTICLE INFO

Keywords:
Titanium dioxide
Colorectal cancer
Transcriptomics
Mouse colon
Nanomaterials
Food additive E171

ABSTRACT

Dietary factors that may influence the risks of colorectal cancer, including specific supplements, are under investigation. Previous studies showed the capacity of food additive titanium dioxide (E171) to induce DNA damage *in vitro* and facilitate growth of colorectal tumours *in vivo*. This study aimed to investigate the molecular mechanisms behind these effects after E171 exposure. BALB/c mice were exposed by gavage to 5 mg/kg$_{bw}$/day of E171 for 2, 7, 14, and 21 days. Transcriptome changes were studied by whole genome mRNA microarray analysis on the mice's distal colons. In addition, histopathological changes as well as a proliferation marker were analysed. The results showed significant gene expression changes in the olfactory/GPCR receptor family, oxidative stress, the immune system and of cancer related genes. Transcriptome analysis also identified genes that thus far have not been included in known biological pathways and can induce functional changes by interacting with other genes involved in different biological pathways. Histopathological analysis showed alteration and disruption in the normal structure of crypts inducing a hyperplastic epithelium. At cell proliferation level, no consistent increase over time was observed. These results may offer a mechanistic framework for the enhanced tumour growth after ingestion of E171 in BALB/c mice.

1. Introduction

Colorectal cancer (CRC) in industrialized countries is the 3rd cancer in men and the 2nd in women with a total of 694,000 deceased people in 2012 (8.5% of all cancer deaths that year) (Globocan, 2012). Obesity, alcohol, and tobacco smoking are factors that may increase the risk of developing CRC whereas fruits and vegetables have been shown to be associated with decreased risk of CRC. Most likely as a consequence of their high fibre content and the presence of a wide range of bioactive compounds, including antioxidant (de Kok et al., 2010; Haggar and Boushey, 2009).

The increased incidence of CRC has been observed particularly in industrialized countries over the last decades and could potentially be explained by specific dietary patterns such as Western types of diets (Globocan, 2012).

Colouring agents are used in many different types of food. Titanium dioxide (TiO_2) is used as a colouring agent (EU, 2012), it gives a white colour to food products such as salad dressings, chewing gum, icing, cookies and candies (Peters et al., 2014; Weir et al., 2012). Following a risk assessment performed by the joint Food and Agriculture Organization/World Health Organization (FAO/WHO), TiO_2 was approved as a food additive in 1969 by the European Union under the name of E171 (EU, 2012). It is permitted in food at *quantum satis*, which indicates that there is no maximum level specified. In 2010, the International Agency for Research in Cancer (IARC) classified TiO_2 as possible carcinogen to humans (Group 2B) mainly based on inhalation studies *in vivo* as well as epidemiological studies on effects of exposure to microparticles (MPs) and nanoparticles (NPs) of TiO_2 (IARC, 2010).

E171 consists of approximately 40% of TiO_2 NPs (< 100 nm) and 60% of TiO_2 MPs (> 100 nm) (Dorier et al., 2017; Proquin et al., 2017a; Weir et al., 2012). In the USA, the estimated average exposure of children below 10 years of age was 1–2 mg TiO_2/kg$_{bw}$/day and above 10 years old, 0.2–0.7 mg TiO_2/kg$_{bw}$/day. In the UK, the estimated exposure was on average 2–3 mg TiO_2/kg$_{bw}$/day for children younger than 10 years and 1 mg TiO_2/kg$_{bw}$/day for children over 10 years of age (Weir et al., 2012). Another study performed in the Netherlands showed an intake of TiO_2 in the same range as in the USA (Rompelberg et al., 2016). This study, published in 2016, estimated the mean average

* Corresponding author. Department of Toxicogenomics, Maastricht University, P.O. Box 616, 6200 MD Maastricht, The Netherlands.
E-mail address: h.proquin@maastrichtuniversity.nl (H. Proquin).

https://doi.org/10.1016/j.fct.2017.11.011
Received 5 July 2017; Received in revised form 20 October 2017; Accepted 7 November 2017
Available online 08 November 2017
0278-6915/ © 2017 Elsevier Ltd. All rights reserved.

Abbreviations

AOM	Azoxymethane
AU	Arbitrary Units
CPDB	Consensus Pathway DataBase
CRC	Colorectal cancer
DEG	Differentially Expressed Genes
DSS	Dextran Sodium Sulphate
EFSA	European Food Safety Authority
FES	Feature Extraction Software
GSEA	Gene Set Enrichment Analysis
GPCR	G-Protein Coupled Receptor
H&E	Hematoxylin & Eosin
LIMMA	Linear Mix Model Analysis for Microarrays
MPs	Microparticles
NPs	Nanoparticles
ORA	Over-Representation gene set Analysis
PBS	Phosphate-Buffered Saline
RIN	RNA Integrity Number
ROS	Reactive Oxygen Species
TiO_2	Titanium dioxide

exposure to be 0.67 mg TiO_2/kg_{bw}/day between 2 and 6 years old, 0.17 mg TiO_2/kg_{bw}/day between 7 and 69 years old and 0.06 mg TiO_2/kg_{bw}/day above 70 years old. Furthermore, in June 2016, a new evaluation from the European Food Safety Authority (EFSA) on TiO_2 in food was published (EFSA, 2016). In the non-brand-loyal scenario validated by the EFSA, it has been estimated that the mean exposure ranged from 0.2 mg/kg_{bw}/day for infants and the elderly to 5.5 mg/kg_{bw}/day for children. At the 95th percentile, EFSA estimates the exposure ranged from 0.5 mg/kg_{bw}/day for the elderly to 14.8 mg/kg_{bw}/day for children.

Although some studies report no adverse effects of TiO_2 (Macwan et al., 2011) many others indicate adverse effects of MPs and NPs of TiO_2. These effects are diverse and have been observed *in vivo* as well as *in vitro*. It includes gene expression changes related to immune response and inflammation in mice exposed intragastrically to 10 mg/kg_{bw} for 90 days (Cui et al., 2015). After whole genome microarray analysis in mice livers, Cui et al. observed the generation of inflammation and a reduction in immune capacity by the downregulation of genes involved in the complement system. These results are in line with a recent study on the effects of ingestion of 10 mg/kg_{bw} of E171 for 7 and 100 days in rats (Bettini et al., 2017). In the rats' Peyer's Patches, a significant decreased frequency of immunoregulatory Tregs and $CD4^+CD25^+$ T helpers was observed after 7 and 100 days. Furthermore, induction of inflammatory markers such as TNF-α, IL-8 and IL-10 was measured in aberrant crypts after 100 days of exposure to E171. A potent Th1/Th17 immune response was detected via an increased production of IFN-γ in Peyer's Patches and IFN-γ and IL-17 in the spleen after 7 days of exposure. Another *in vivo* study observed a reduction in both non-specific and specific immune responses in rats' primary pulmonary alveolar macrophages exposed by inhalation to TiO_2 NPs (5 and 200 nm; 0.5, 5, or 50 mg/kg_{bw}) (Liu et al., 2010). Additionally, TiO_2 NPs have an impact on the bacterial ratio of the human intestinal community *in vitro* which can affect the immune response (Dudefoi et al., 2017). Inflammation is enhanced via the production of reactive oxygen species (ROS). In an *in vitro* study, oxidative stress was produced by E171 and TiO_2 NPs in a cell-free environment whereas MPs induced ROS formation in the presence of Caco-2 cells (Proquin et al., 2017a). These results confirmed previous studies in which ROS production was observed in mouse fibroblasts and fish cells with fibroblast-like morphology (Jin et al., 2008; Reeves et al., 2008) and *in vivo* in mice exposed intragastrically to TiO_2 NPs for 60 days (Cui et al., 2010). The findings of this mouse study showed a significant increase of $O_2^{\bullet -}$ and H_2O_2 in the liver starting at a concentration of 10 mg/kg_{bw}. ROS production can lead to DNA damage in mice but also in human cells like liver hepatocellular cells (HepG2) and bronchial epithelial cells (BEAS-2B) (Chen et al., 2014; Park et al., 2008; Shi et al., 2015; Zijno et al., 2015). Recently we have demonstrated that E171 as well as NPs and MPs of TiO_2 possess the capacity to induce single-strand DNA damage in Caco-2 cells and induce micronuclei in HCT116 cells (Proquin et al., 2017a).

A reduction of the immune capacity, induction of inflammation and DNA damage can increase the risk of developing cancer. An *in vivo* study performed in BALB/c mice in which CRC was chemically induced by a combination of azoxymethane (AOM) and dextran sodium sulphate (DSS) showed, after 10 weeks of ingestion of 5 mg/kg_{bw}/day of E171, a significantly increased number of tumours in the colon as compared to the control (AOM/DSS) (Urrutia-Ortega et al., 2016). It was concluded that E171 exacerbates the number of tumours induced by a genotoxic insult in addition to an irritant. In absence of AOM/DSS, mice did not develop tumours. However, the exposure of mice to E171 only induced hyperplastic epithelium with dysplastic changes with an increase of crypts size and number, and a decrease in the number of goblet cells in the colon of mice. In addition, staining for tumour progression markers showed a significant increase of COX2, Ki67 and β-catenin markers.

In order to understand the molecular changes behind these phenotypical modifications, and behind the production of ROS and DNA damage *in vitro*, a new experiment was designed. Physiological changes were previously observed from 4 weeks on (Urrutia-Ortega et al., 2016), therefore the exposure time was limited to 3 weeks. To establish responses to E171 exposure at the mRNA level in the colon of BALB/c mice, mice ingested 5 mg/kg_{bw}/day of E171 for 2, 7, 14, and 21 days. Transcriptome changes were determined by whole genome mRNA microarrays. Moreover, histological changes were studied by Hematoxylin & Eosin (H&E) and a proliferation marker (Ki67) staining. We hypothesized that the exposure to E171 induces inflammatory, immunological and specific cancer-related pathways in colon tissue that may explain the facilitated development of CRC by E171 reported previously.

2. Materials and methods

2.1. E171 particle characterization

E171 was kindly donated by the Sensient Technologies Company in Mexico. E171 was previously characterized by electron microscopy with Scios DualBeam FIB/SEM (SEM, 20 KV, The Netherlands) at 150,000× magnification to evaluate the size and morphology. To evaluate the hydrodynamic size distribution and the zeta potential a Malvern Nano ZS (Malvern Instruments, UK) dynamic light scattering instrument was used. Results have been previously published (Proquin et al., 2017a). E171 comprises 2 fractions of different sizes with a ratio of 39% NPs and 61% MPs. E171 contains slightly to fully rounded particles. At non cytotoxic concentration, the dynamic size of E171 was 316.8 ± 282.4 d.nm and the zeta potential −12.78 ± 0.52 mV.

2.2. Mouse model

BALB/c mice underwent exposure to E171 by ingestion at the Unidad de Biomedicina, Facultad de Estudios Superiores Iztacala, Universidad Nacional Autónoma de México, Mexico. Experiment was approved by the Comité de Ética de la Facultad de Estudios Superiores Iztacala de la Universidad Nacional Autónoma de México under the number: FESI-ICY-I151. Experimental work followed the guidelines of Norma Oficial Mexicana (NOM-062-ZOO-1999, NOM-087-ECOL-1995) and the Protocol for the Care and Use of Laboratory Animals (PICUAL).

Thirty-two BALB/c mice (16 males, 16 females) of 4–6 weeks old (Harlan Laboratories, Mexico) were housed in polycarbonate cages and kept in a housing room (21°C, 50–60% relative humidity, 12 h light/dark cycles, air filtered until 5 μm particles and was exchanged 18 times/h). The number of animals was determined with a power calculation. The calculation was performed with a web-based source named Power Atlas (http://poweratlas.ssg.uab.edu/). It was created by Gadbury et al. and Page et al. to assist researchers in the planning and design of microarray and expression based experiments (Gadbury et al., 2004; Page et al., 2006). This software is currently aimed at estimating the power and sample size for a two groups comparison based upon pilot data. The results of this calculation showed that with 16 animals per exposure group and an alpha at 0.1, the power of the experiment is over 80%. Standard commercial rat chow diet from Harland Teklad (Madison, WI, USA) was given *ad libitum* as well as water. After one week of acclimation, the mice were randomly divided in the following groups: a) control (8 males, 8 females), b) E171 group (8 males, 8 females). Both the control and exposure groups received a single intraperitoneal injection of 500 μL of sterile saline solution a week before the start of the experiment and water *ad libitum* between day 1 and 5 respectively. This was to mimic comparable conditions but now without an AOM injection and the supply of DSS in drinking water given in the CRC model. One milligram of E171 was sterilized, resuspended in 1 mL of water and sonicated for 30 min at 60 Hz. The E171 group of mice received an intragastric administration of 5 mg/kg body weight of E171 by a gavage from Monday to Friday during 21 days according to the scheme (Fig. 1). The control group received 100 μL of sterile sonicated water (30 min at 60 Hz) by intragastric gavage from Monday to Friday during 21 days according to the scheme. After 2, 7, 14, and 21 days, 4 mice (2 males, 2 females) were sacrificed in a humid chamber with sevoflurane and colon was collected. Colons were directly put in a tube containing RNA*later*® (Thermofischer, The Netherlands) and left overnight at 4 °C. Next day the remaining RNA*later*® was discarded. The organs were stored at −80°C until RNA isolation. The samples have been transported in dry ice at −80°C for 2 days. The temperature of the samples has been monitored throughout the shipping process with a thermometer provided by the shipping company to ensure stable freezing conditions and optimal sample quality. Samples have been put at −80°C in the freezer immediately upon arrival. RNA isolation and further procedures were performed at the Department of Toxicogenomics, Maastricht University, Maastricht, the Netherlands.

2.3. mRNA isolation from distal colons

The previous study from our group showed an increased numbers of tumours in the distal colon of BALB/c mice (Urrutia-Ortega et al., 2016), therefore it was chosen to isolate total RNA from this part of the colon. Before RNA isolation, the distal colon was submerged in Qiazol (Qiagen, The Netherlands) and subsequently disrupted and homogenized using a Mini Bead Beater (BioSpec Products, The Netherlands) on a speed of 48 beats per second for 30 s. Isolation of RNA was performed using the miRNeasy Mini Kit (Qiagen, The Netherlands) including a DNase treatment, according to the manufacturer's protocols for “Animal Cells and Animal Tissues” (Qiagen, 2012). The concentration of total RNA was measured on a Nanodrop® ND-1000 spectrophotometer (Thermofischer, The Netherlands). The integrity of total RNA was checked using RNA Nanochips on a 2100 Bioanalyzer (Agilent Technologies, The Netherlands). Only samples with an RNA Integrity Number (RIN) higher than 6 were used for microarray analysis which was the case for all samples with an average of 8.8 ± 0.7.

2.4. cRNA synthesis, labelling and hybridization

Total RNA was synthesized into cRNA and labelled according to the One-Colour Microarray-Based Gene Expression Analysis protocol version 6.6 (Agilent Technologies, The Netherlands). The procedure was performed as described by the manufacturers protocol (Agilent, 2015). The RNeasy Mini Kit (Qiagen, The Netherlands) was used to purify the amplified cRNA samples according to the manufacturer's protocol of Agilent. Subsequently, the cRNA was quantified using a Nanodrop® ND-1000 spectrophotometer with a Microarray Measurement. The yield and specific efficiency of the labelling of the cRNA was determined using the formulas in the protocol of Agilent.

Hybridization was performed according to the Agilent's protocol on SurePrint G3 mouse Gene exp 60kv2 microarrays slides (Agilent Technologies, The Netherlands). After hybridization, the microarray slides were scanned using an Agilent DNA Microarray Scanner with Surescan High-resolution Technology (Agilent Technologies, The Netherlands) with scanner settings to Dye Channel: G, Profile: AgilentG3_GX_1Colour, Scan region: Agilent HD (61 × 21.3 mm), Scan

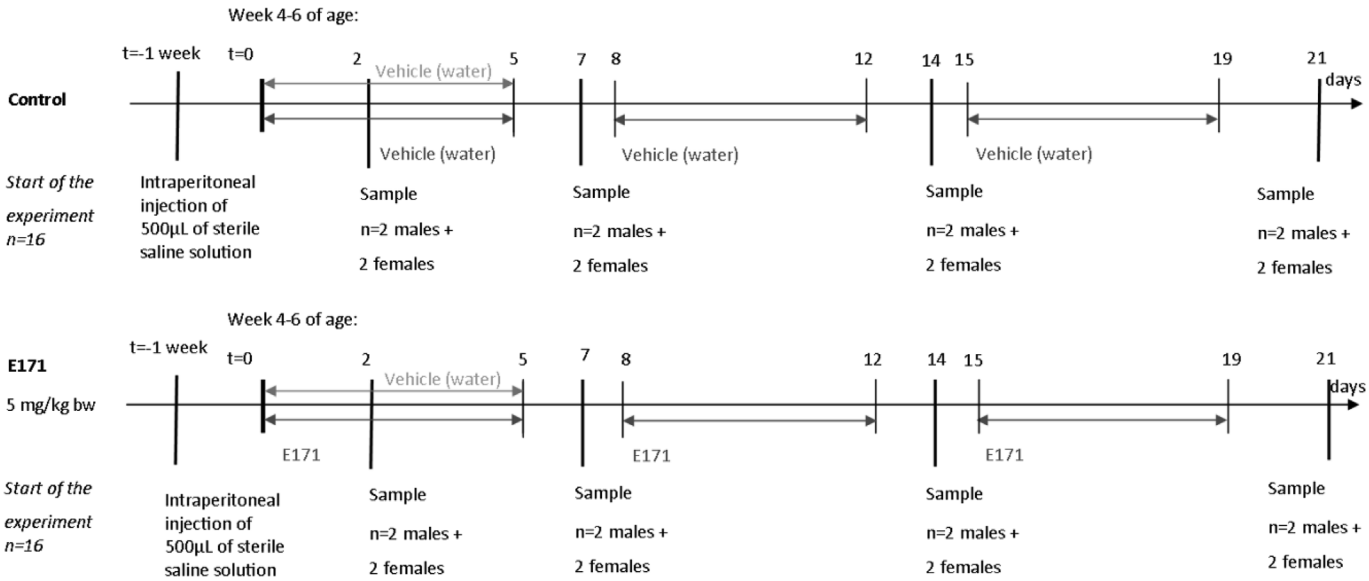

Fig. 1. Scheme of exposure of experimental mouse model. BALB/c mice (n = 32) were randomly distributed in 2 groups: one control group with water as a vehicle (dark grey line) and one exposure group with E171 (dark grey line). Both groups received a single intraperitoneal injection of 500 μL of sterile saline solution a week before the start of the experiment (t = −1 week vertical line) and water *ad libitum* between day 1 and 5 respectively (light grey line). This was to mimic comparable conditions but now without an AOM injection and the supply of DSS in drinking water given in the CRC model. Vertical lines correspond to the sampling times at 2, 7, 14, and 21 days.

resolution 3 μm, Tiff file dynamic range: 20 bit, Red PMT gain: 100%, Green PMT gain: 100%.

2.5. Pre-processing and data analysis of microarrays

The methods for pre-processing were performed as previously described (Espin-Perez et al., 2015). In short, first the quality of the microarrays was checked by the quality control pipeline provided by Agilent (Feature extraction software (FES) version 10.7.3.1). All samples met the quality criteria of the FES. In order to have a thorough quality check and normalize the data with local background correction, flagging of bad spots, controls and spots with too low intensity, log2 transformation and quantile normalization an in-house QC pipeline was developed and is publically available (github.com/BiGCAT-UM/arrayQC_Module). All samples met the in-house quality check. Raw data with expression values and genes were selected for data analysis based on flags and missing values (GEO accession: GSE92563). Height groups were defined: E171 2 days, 7 days, 14 days, 21 days for the exposed samples and control 2 days, 7 days, 14 days, 21 days for the controls. Within each group, at least 66% of the samples had to have a pass for the spot. Also, within each group, unique spot identifiers passed when there were less than 40% of missing values. The unique spot identifiers with an average expression less than four in all of the groups were omitted. The missing values were pre-processed using the GenePattern ImputeMissingValues.KNN module v13 (Reich et al., 2006), with standard settings. Unique spot identifiers were removed and identical Agilent probe identifiers were merged with Babelomics 5 (Alonso et al., 2015), using the median method for pre-processing data. Next, the data was re-annotated from Agilent probe identifiers to EntrezGene identifiers (EntrezGeneIDs). The expression data for all genes with an identical EntrezGeneIDs were subsequently merged with Babelomics 5, using the median method for pre-processing data. Using an R-script, a Linear Mixed Model Analysis for Microarrays (LIMMA) (Smyth, 2017) (version 1.0) was performed to extract differentially expressed genes (DEG) (Smyth, 2005). The data of each control time point (control) was subtracted from the time-matched exposed mice to E171. The standard cut-off values of a fold-change (FC) of 1.5 and a p-value of 0.05 were used in LIMMA. Furthermore, the false discovery rate was calculated according to the Benjamini-Hochberg method with a threshold at 0.05.

2.6. Pathway and network analyses

The DEG for each time point were subsequently used in Consensus Pathway Database (CPDB) for an over-representation gene set analysis (ORA) (Herwig et al., 2016; Kamburov et al., 2013). CPDB is an aggregate of 16 different databases developed by the Max Planck institute (Herwig et al., 2016). With respect to content, CPDB has a focus on molecular interactions, and it provides deep exploration of the interactome network, protein complexes and pathway resources. All the available databases from CPDB were used (release MM9, 11 Oct. 2013) with settings in the “pathways as defined by pathway databases” with a minimum overlap of input list of 2 and a p-value cut-off of $p < 0.01$. For computing the significance of the over-representation of the annotation sets with respect to user-input molecules, CPDB applies Fisher's exact test. For each annotation set, the p-value is calculated. As many annotation sets are tested, CPBD corrects for multiple hypothesis testing using the false discovery rate procedure within each type of annotation set (Herwig et al., 2016; Kamburov et al., 2013).

To validate the ORA method, a gene set enrichment analysis (GSEA) was performed. The GSEA method performed by CPDB carries out a paired Wilcoxon signed-rank test for each pathway based on the measurement values of each DEG per time point (Herwig et al., 2016; Kamburov et al., 2013). All available databases from CPDB were used with settings in the “pathways as defined by pathway databases” with a minimum number of measured genes of 4 and a p-value cut-off of $p < 0.01$.

A network analysis was performed using Cytoscape (version 3.4.0) (Cline et al., 2007) with the software application Genemania (version 3.4.1). The Genemania plugin in Cytoscape is based on a guilt-by-association approach to derive predictions from a combination of potentially heterogeneous data sources. The integration of an association of networks from multiple sources into a single composite network using a conjugate gradient optimization algorithm as described in Mostafavi et al. (2008). Networks are weighted according to query dependent criteria. This compact matrix representation is used directly by the conjugate gradient algorithm. Genemania allows the connection of genes in a network based on information on their function and expression found in literature (Montojo et al., 2010), all DEG per time point were used and compared to the GEO database of *Mus musculus* for co-expression. The network was built using the EntrezGeneID. Among the 417 DEG at 2 days of exposure, 196 could not be recognized by Genemania, 221 could be included in the network and 20 were added by GeneMania to improve the connections between the genes. Among the 971 DEG at 7 days of exposure, 271 could not be recognized by Genemania, 700 could be included in the network and 20 were added by GeneMania. Among the 1512 DEG at 14 days of exposure, 336 could not be recognized by Genemania, 1176 could be included in the network and 20 were added by GeneMania. Among the 229 DEG at 21 days of exposure, 90 could not be recognized by Genemania, 140 could be included in the network and 19 were added by GeneMania. DEG belonging to a known pathway were extracted from the network, separated per biological processes (e.g. signalling, immune response) and coloured. All genes added by Genemania to improve the network by linking some genes together were labelled with a different symbol and colour and were also extracted from the network.

2.7. Colorectal histology and Ki67 proliferative cell marker

The distal part of the colon was dissected, extensively washed with PBS and fixed with 4% paraformaldehyde. After fixation, colons were dehydrated in ethanol and embedded in paraffin. Cuts of 5 μm thickness were stained with Hematoxylin (Sigma-Aldrich, Mexico) & Eosin (Sigma-Aldrich, Mexico).

Ki67 immunostaining was used as a proliferative cell marker. Briefly, tissue section of 5 μm thickness were permeabilized and incubated overnight with primary antibody (dilution 1:300). Samples were then washed with PBS and incubated with the secondary antibody (dilution 1:100; IgG-FITC, Santa Cruz) for 1.5 h at 37°C. Samples were analysed using a LEICA TCS SP2 confocal microscope. In each sample, 20 fields of 50 square millimetres were randomly used for fluorescence quantification. Data are described as mean ± standard error. Statistical analysis was performed with a Student t-test.

3. Results

3.1. Differently expressed genes (DEG)

DEG were observed per time point after correction by the time-matched control, indicating the impact of E171 on the gene expression levels in the distal colon.

The number of genes that passed the pre-processing in all time points was 21,106 genes, of which 417 were significantly different ($p < 0.05$ and $FC > 1.5$) after 2 days of exposure, 971 after 7 days, 1512 after 14 days and 229 after 21 days (Table 1). Using an adjusted p-value, no DEG were observed at 2 and 21 days, therefore, the criteria for DEG used for further analysis are $p < 0.05$ and $FC > 1.5$.

The majority of the genes was time specific, whereas a small number was in common between several time points (Fig. 2) and only one gene was significantly upregulated at all time points: Cyfip1 (Supplementary Fig. 1). In total 32 DEG were in common between 3 out of 4 time points. Of these, 11 DEG were in common between time points 2, 7, and 14 days however only 6 had a known biological function, others were

Table 1
Summary of results of DEG after LIMMA analysis.

	2 days	7 days	14 days	21 days
|FC| > = 1.5	1593	2638	3057	1305
Upregulated	776	717	823	520
Downregulated	817	1921	2234	785
p.val < 0.05	922	1918	3395	545
adj.p.val < 0.05	0	8	385	0
|FC| and p.val	417	971	1512	229
|FC| and adj.p.val	0	7	289	0

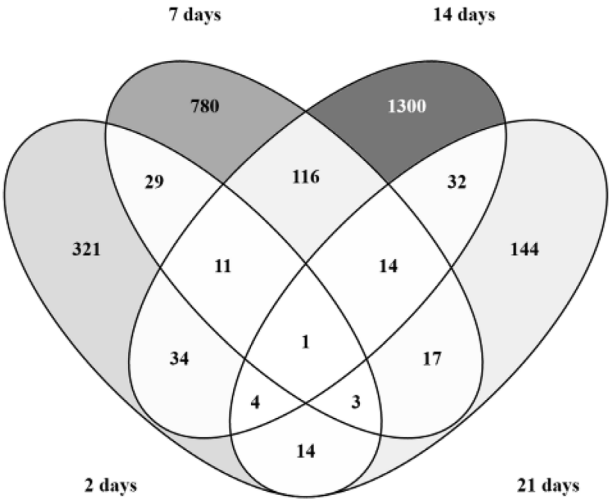

Fig. 2. Venn diagram showing the overlap of DEG (p < 0.05 and FC > 1.5) between the different time points (2, 7, 14, and 21 days) after exposure to E171 in colon of mice. Grey scale indicates the number of genes in the different parts of the Venn diagram.

cDNA or genes without a known function. This was also observed in the cluster with 7, 14, and 21 days where 13 DEG out of 14 had a known function. The 2, 7, and 21 days cluster contained 1 known DEG out of 3. The 2, 14, and 21 days cluster had 2 known DEG out of 4. Finally, there was a total of 23 DEG with a known biological function in 3 out of 4 time points and 1 common in the 4 time points. The gene names and direction of expression of the genes are shown in Supplementary Fig. 1.

3.2. Pathway and network analyses per time point

To gain insight in biological mechanisms of effects of E171, pathways were identified based on the CPDB as described in the Materials and Methods section. Only a relatively low proportion of the full list of DEG was involved in specific molecular pathways and could be identified by CPDB. Therefore, a network analysis with co-expression of genes was performed in order to observe the connection between genes in pathways and those that are as yet not included in these pathways. This allows for an improved and more complete biological interpretation of the effect of E171 in the colon. Below, first the results of the pathways analysis are described, followed by the network analysis.

3.2.1. Pathway analysis

3.2.1.1. 2 days of exposure. In Table 2, pathways identified per time point after ORA in CPDB are presented. After 2 days of exposure, signalling pathways such as signalling by GPCR, GPCR downstream signalling and signal transduction were observed. Furthermore in the same family as GPCRs, DEG were regulated in molecular pathways such as olfactory signalling, olfactory transduction and odorant GPCRs. More details about the fold change and the direction of expression of the genes are presented in Table 5, in ref (Proquin et al., 2017b).

A second group of pathways corresponded to an immune response with pathways such as Epstein-Barr virus infection and antigen processing and presentation. These 2 pathways contained genes such as H2-M9, Hspa1b and Hspa1a, Polr2d which were downregulated whereas Ikbkb, Cdkn1a and H2-M11 were upregulated.

In a third group of pathways, cancer signalling group, 2 pathways were modulated: MAPK signalling pathway and destabilization of mRNA by AUF1 (hnRNP D0).

In the last group, metabolism, the Protein processing in endoplasmic reticulum pathway consisted of only down-regulated DEG such as Dnaja1, Dnajb1 and Ube2g2 (Table 5, in ref [Proquin et al., 2017b]).

The activation of signalling genes was confirmed by GSEA which resulted in 5 signalling pathways after 2 days of exposure (Supplementary Table 1). All pathways were common to the ORA and contained the same genes.

3.2.1.2. 7 days of exposure. The results after ORA showed that at day 7 of exposure and comparable to 2 days of exposure, signalling pathways were observed such as olfactory, GPCR, and signal transduction pathways, and insulin events with downregulated genes such as Ins1, Prkag3 and Trib3. The p-value of the signalling pathways were from 10^{-4} to 10^{-15} (Table 2). In the identical signalling pathways between 2 and 7 days, the number of DEG at 7 days was increased compared to 2 days. Also the ratio up- and -downregulated genes was increased towards up-regulation. More details about the genes can be found in Table 6, in ref (Proquin et al., 2017b).

As at day 2 of exposure, after 7 days, a group of pathways related to cancer signalling was observed and contained a pathway linked to the MAPK pathway; p38MAPK event. Other pathways in cancer signalling at 7 days were no longer common to 2 days and contained some interesting upregulated genes such as Trp53, Mapkap3, Hist4h4Apc, Fzd5, and Patch1.

Compared to 2 days, new pathways were related to oxidative stress. These pathways contained upregulated genes such as Phc1, Tpr3 (synonym of Tp53) and histone clusters.

A second newly identified group of pathways named cell cycle with pathways such as RNA Polymerase I Promoter Opening pathway contained upregulated histone cluster genes.

Furthermore, a neuronal system group of pathways contained amyloids and meiotic synapsis pathways with some upregulated histone genes.

In addition, genes in metabolism pathways were modulated and ranging from vitamin C metabolism to protein citrunillation. The latter contained 2 downregulated DEG; Padi1 and Padi2.

As well as at day 2, at day 7, the activation of signalling genes was confirmed by using the GSEA method. Five of the 7 olfactory pathways were also observed and contained the same genes (Supplementary Table 1).

In relation to the RNA polymerase pathway, mRNA processing pathway was present after using the GSEA method. This pathway contained genes related to the translation of mRNA with genes such as Eif4g3, Taf15, Papolg and Rbm6.

A pathway related to the transmembrane transport of small molecules was observed only after GSEA, with 14 genes from the solute carrier family.

3.2.1.3. 14 days of exposure. The ORA showed that, after 14 days of exposure, 22 pathways illustrated the effect of E171 (Table 2). More details about the genes can be found in Table 7, in ref (Proquin et al., 2017b).

Like at day 2 and 7, at day 14 a group of cancer signalling pathways was identified although the pathways included in that group were not identical. The pathways at day 14 were mostly related to the PI3K/AKT activation but also Glioma, Melanoma and GAB1 signalosome. Some of these genes were of interest such as downregulation of Pten or upregulation of Pik3r2, Akt1s1, Pik3r1, Foxo3, Src, Cdkn1a, Trp53 and Akt2.

Immune related genes were expressed in the same direction as at

Table 2
Result of the pathway over-representation analysis of the DEG in the distal colon of BALB/c mice after exposure to E171.

Time of exposure	Group of pathways	Name of pathway	p-value	Database
2 days	Signalling	- Olfactory transduction	7.36E-10	KEGG
		- Olfactory Signalling Pathway	9.95E-06	Reactome
		- Odorant GPCRs	8.67E-05	Wikipathways
		- Signalling by GPCR	0.000288	Reactome
		- GPCR downstream signalling	0.00052	Reactome
		- Signal Transduction	0.00745	Reactome
	Immune response	- Epstein-Barr virus infection	0.00632	KEGG
		- Antigen processing and presentation	0.00673	KEGG
	Cancer signalling	- Destabilization of mRNA by AUF1 (hnRNP D0)	0.00239	Reactome
		- MAPK signalling pathway	0.00473	KEGG
	Metabolism	- Protein processing in endoplasmic reticulum	0.00848	KEGG
7 days	Signalling	- Olfactory transduction	1.03E-15	KEGG
		- Olfactory Signalling Pathway	1.86E-12	Reactome
		- GPCR downstream signalling	3.99E-10	Reactome
		- Signalling by GPCR	1.39E-09	Reactome
		- Signal Transduction	1.03E-07	Reactome
		- Odorant GPCRs	0.000703	Wikipathways
		- GPCRs, Other	0.000938	Wikipathways
		- IRS-related events	0.00283	Reactome
		- Insulin receptor signalling cascade	0.00439	Reactome
		- SHC activation	0.00463	Reactome
	Cancer signalling	- Cellular Senescence	0.00301	Reactome
		- Basal cell carcinoma	0.0043	KEGG
		- p38MAPK events	0.00817	Reactome
		- Activation of PKB	0.00902	Reactome
		- Formation of Senescence-Associated Heterochromatin Foci (SAHF)	0.00902	Reactome
	Cell cycle	- Meiosis	0.00361	Reactome
		- Meiotic Recombination	0.00488	Reactome
		- RNA Polymerase I Promoter Opening	0.00599	Reactome
	Oxidative stress	- Oxidative Stress Induced Senescence	0.00409	Reactome
		- Cellular responses to stress	0.00826	Reactome
	Neuronal system	- Amyloids	0.00488	Reactome
		- Meiotic Synapsis	0.00272	Reactome
	Metabolism	- Vitamin C (ascorbate) metabolism	0.00195	Reactome
		- protein citrullination	0.00902	MouseCyc
14 days	Cancer signalling	- GAB1 signalosome	0.0029	Reactome
		- PIP3 activates AKT signalling	0.00535	Reactome
		- PI-3K cascade	0.00535	Reactome
		- PI3K events in ERBB2 signalling	0.00535	Reactome
		- PI3K events in ERBB4 signalling	0.00535	Reactome
		- PI3K/AKT Signalling in Cancer	0.00535	Reactome
		- PI3K/AKT activation	0.00723	Reactome
		- Glioma	0.00777	KEGG
		- Melanoma	0.00868	KEGG
		- Constitutive PI3K/AKT signalling in Cancer	0.00882	Reactome
	Cell cycle	- Caspase-mediated cleavage of cytoskeletal proteins	0.00608	Reactome
		- Signalling by ERBB4	0.00795	Reactome
		- PERK regulated gene expression	0.00435	Reactome
	Oxidative stress	- Mitochondrial Uncoupling Proteins	0.00435	Reactome
		- The fatty acid cycling model	0.00435	Reactome
		- The proton buffering model	0.00435	Reactome
	Immune response	- Role of LAT2/NTAL/LAB on calcium mobilization	0.00359	Reactome
		- Chemokine signalling pathway	0.00829	KEGG
		- Role of phospholipids in phagocytosis	0.00392	Reactome
	Bone development	- Chondroitin sulfate biosynthesis	0.00514	Reactome
		- Chondroitin sulfate/dermatan sulfate metabolism	0.00844	Reactome
	Neuronal system	- Serotonin receptors	0.00493	Reactome
21 days	Signalling	- Olfactory Signalling Pathway	0.00035	Reactome
		- Olfactory transduction	0.000556	KEGG
		- GPCR downstream signalling	0.00162	Reactome
		- Signal Transduction	0.00453	Reactome
		- Signalling by GPCR	0.00543	Reactome
	Oxidative stress	- Mitochondrial Uncoupling Proteins	7.71E-05	Reactome
		- The fatty acid cycling model	7.71E-05	Reactome
		- The proton buffering model	7.71E-05	Reactome
	Metabolism of proteins	- Synthesis of glycosylphosphatidylinositol (GPI)	0.00655	Reactome

day 2 with different pathways such as role of LAT2/NTAL/LAB on calcium mobilization, chemokine signalling pathway and role of phospholipids in phagocytosis.

Modulation of genes in the group of cell cycle pathway was common to 7 days of exposure with different pathways such as caspase-mediated cleavage of cytoskeletal proteins, signalling by ERBB4 and PERK regulated gene expression. In the cell cycle group and the immune system group approximately 1/3 of the DEG were upregulated.

Oxidative stress genes were activated as well as after 7 days of exposure but different pathways were involved in this activation. Interestingly, the oxidative stress group included the upregulation of Ucp2 and Ucp3 which were also upregulated at 21 days of exposure.

As well as after 7 days of exposure, genes related to a neuronal response were also activated but with a different pathway, serotonin receptors.

An additional process with genes related to bone development was activated after 14 days of exposure, with 2 pathways being affected.

When the GSEA method was applied, similar results to the ORA were observed which confirms previously observed results. As well as at 7 days of exposure, GSEA displayed the modulation of signalling genes with 7 pathways. Among these 7 pathways, 2 were common to 2 and 7 days of exposure: signal transduction and signalling by GPCR.

A similar but stronger immune response was observed with 7 pathways and 96 DEG involved in innate and adaptive immune system. Among the 96 DEG, 78% of them were down-regulated (Supplementary Table 1).

As after 7 days of exposure, at day 14, GSEA showed an activation of genes related to the mRNA processing pathway. In addition, 2 extra pathways related to cellular processes were present, phagosome and endocytosis (Supplementary Table 1).

Two additional processes were observed after 14 days, metabolism, metabolism of proteins and metabolism of diseases with 2, 2, and 14 pathways respectively. In the metabolism of diseases pathways, 13 pathways contained the same 12 genes as these pathways were all related to Mucopolysaccharidoses diseases.

3.2.1.4. 21 days of exposure. The results after ORA showed that at day 21 of exposure, fewer pathways were modulated (Table 2) compared to 14 days of exposure. Nine pathways were modulated and can be clustered into 3 groups.

First, oxidative stress, common to 7 and 14 days, contained 3 pathways with the same 2 upregulated genes: Ucp2 and Ucp3 which were already observed at 14 days.

Secondly, signalling pathways were significantly affected like at 2 and 7 days of exposure with the activation of pathways such as olfactory, GPCR and signal transduction pathways. Interesting genes in these pathways include Cxcl10, Ccl27a which were also involved in an immune response. All these signalling pathways had more upregulated genes than downregulated ones as seen in Table 8, in ref (Proquin et al., 2017b).

Last, metabolism of proteins contained one pathway, synthesis of glycosylphosphatidylinositol (GPI) pathway with 2 upregulated DEG.

After 21 days of exposure, no pathways were observed using GSEA, the response is more subtle.

3.2.2. Network analysis

A relatively small fraction of the full gene list of DEG was involved in molecular pathways; therefore the next approach was to perform a network analysis with Genemania on Cytoscape for each time point with co-expression of genes (Fig. 3). Indeed, genes that were not directly in the pathways described above were now visualized, including the connection with the genes in pathways. With all DEG of each time point (2, 7, 14, and 21 days) networks analyses were performed. For every time point, more than 50% of all DEG could not be connected to a molecular pathway but could be connected with the genes in these pathways via co-expression. In addition, almost all genes in pathways were directly or indirectly connected via genes added by Genemania to genes that are not known to be involved in pathways.

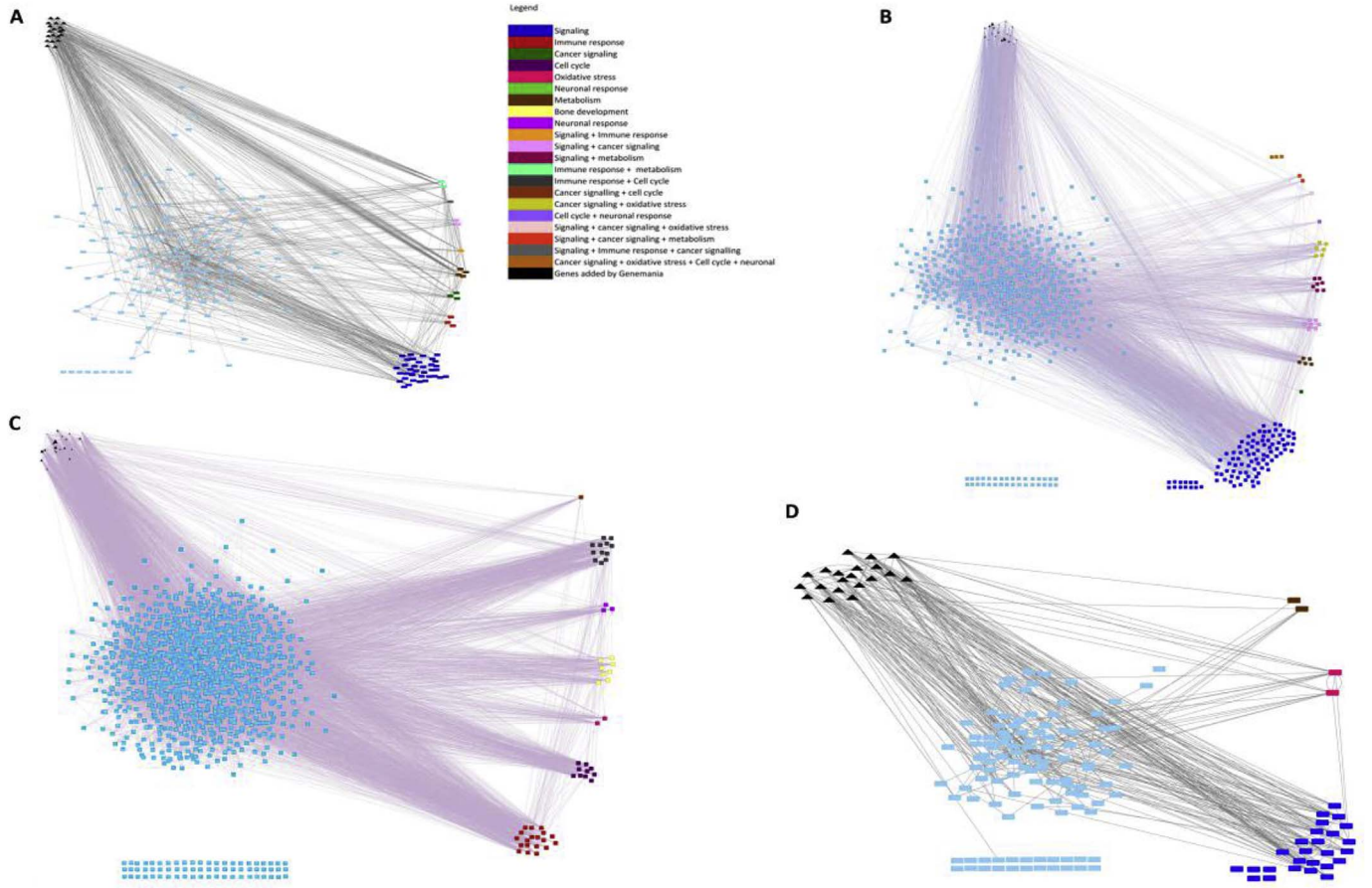

Fig. 3. Linkage of pathway related genes to non-pathway related genes after (A) 2 days, (B) 7 days, (C) 14 days, (D) 21 days of exposure with all pathways $p < 0.01$. All the genes involved in a molecular pathway identified by CPDB after ORA were moved in a half-circle on the right side. Each group of gene has its own colour (see legend) and corresponds to genes involved in one or several biological processes. Genes not included in pathways are in the centre of the figure (light blue rectangles). All the added genes by the GeneMania application were displayed in the upper part of the network (black triangles). Genes that could not be linked in the network are aligned in the bottom left part of the figure (light blue rectangles).

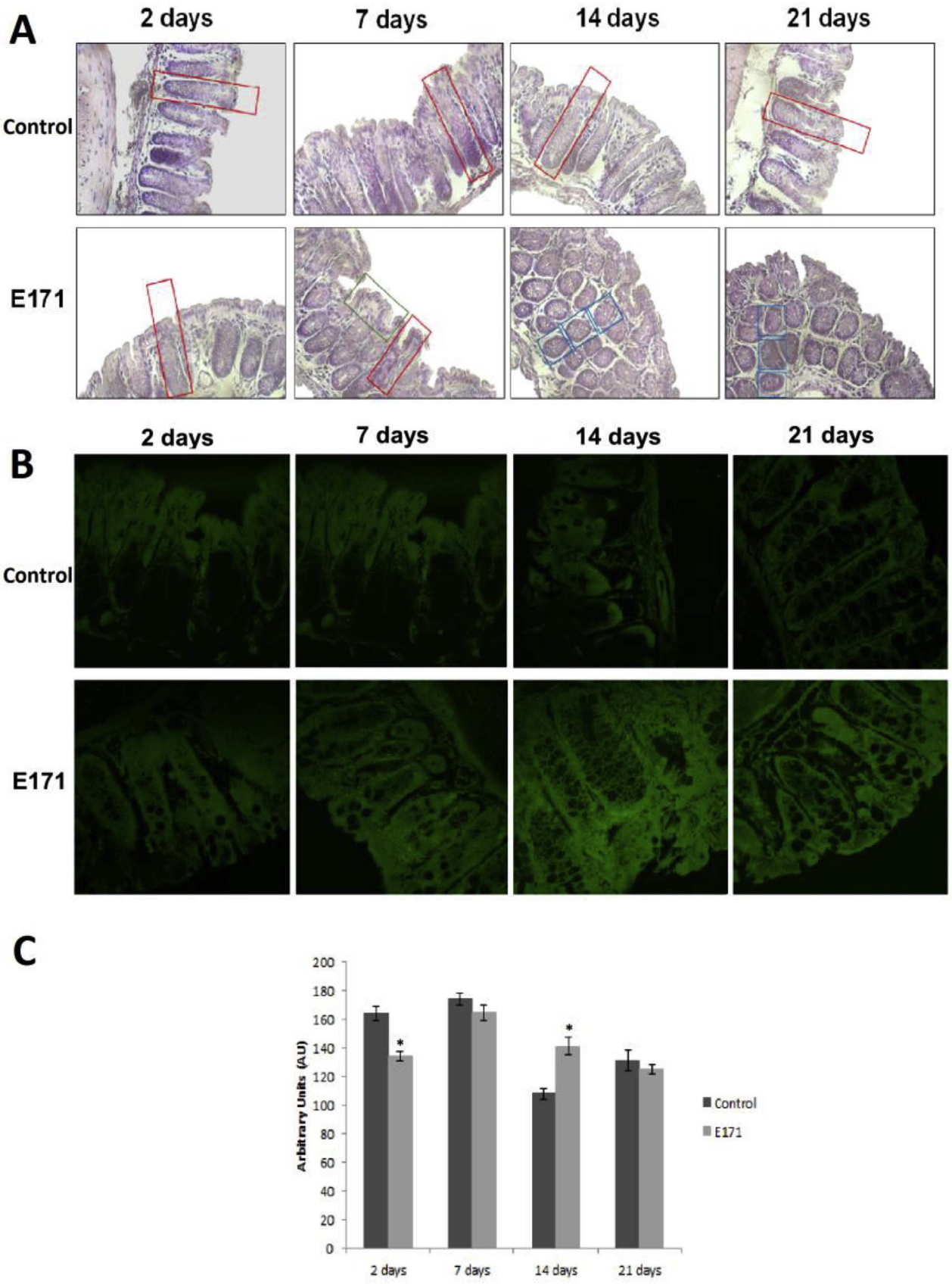

Fig. 4. A) Representative images of histology using H&E staining. Red rectangles show a typical crypt structure in control tissue and also in group exposed to E171 for 2 days. In the exposed group to E171 for 7 days, colon tissue shows seldom alteration of the crypt architecture (green rectangles). Groups from 14 to 21 days of E171 exposure showed hyperplastic epithelium (blue squares). B) Representative images of Ki67 immunodetection of colon tissue of mice exposed to E171 for 2, 7, 14, and 21 days. Images were taken under 63× magnification. C) Arbitrary values of Ki67 immunodetection of colon tissue of control mice and mice exposed to E171. * significant at $p < 0.01$.

Strong interactions between the genes related to molecular pathways and the other DEG can be observed. As these DEG have yet been linked to pathways, the interpretation of the effect of E171 in the colon is limited to the current knowledge about genes included in pathways.

3.3. Colorectal histology and proliferative cell marker

Histological changes were studied after H&E staining on the distal colon of the control group and the group exposed to E171 for all time points (Fig. 4A). The distal colon of control groups showed typical epithelium with normal crypts after 2, 7, 14, and 21 days. Typical structure was also observed in the distal colon of mice treated with E171 for 2 days. However, after 7 days, colon tissue shows seldom alteration of the crypt architecture (green rectangles) and, at a later time point, 14 and 21 days, the exposure to E171 induced disruption in the normal structure of crypts with a hyperplastic epithelium (blue squares).

Expression of Ki67 was analysed in the control group as well as the group exposed to E171 for all the time points (Fig. 4B and C). Results showed that, after 2 days, levels of Ki67 expression is 18% lower in the E171 treated mice compared to its time-matched control (Control: 164.2 ± 40.03 AU, E171: 134.03 ± 26.1 AU, $p < 0.01$). After 7 day of exposure, the Ki67 expression was similar in control and exposed groups. Higher expression of Ki67, increase of 30%, was observed after 14 days in the E171 group compared to the control (Control: 108.27 ± 29.54 AU, E171: 141.4 ± 49.44 AU, $p < 0.01$). As well as at day 7, no differences at day 21 were seen.

4. Discussion

The presented study shows that the food additive E171 induces gene expression changes in the colon of mice that were intragastrically exposed to this compound. Modulations of genes were observed in many different pathways from signalling to metabolism. However, these findings point towards inflammatory, immune, and carcinogenic processes and may offer a mechanistic framework for the enhanced tumour growth after ingestion of E171 in mice treated with AOM and DSS, as observed earlier by our group (Urrutia-Ortega et al., 2016).

Consequent to the early molecular changes detected, seldom alteration of the crypt architecture after exposure to E171 for 7 days and hyperplastic alterations were observed at 14 and 21 days in the distal colon of mice. These results are consistent with the results of a previous study with an identical mouse model performed by our group in which hyperplastic alterations in the colon of mice were observed from 4 weeks of E171 ingestion (Urrutia-Ortega et al., 2016). Histopathological changes in the colon occurred from 7 days on in this study and, in the identical mouse model, an increase of crypts size and number, and a decrease in the number of goblet cells was found from 4 weeks (Urrutia-Ortega et al., 2016). Thus, our results confirm previous studies on the appearance of gene expression alterations before histopathological changes (Castro et al., 2008; Waters and Fostel, 2004).

At the level of cell proliferation after E171 exposure, no consistent increase over time is observed.

With regard to the molecular changes, the common response that we observed over time from 2 to 21 days of exposure (except at 14 days in the ORA) lies in the modulation of genes involved in GPCR and olfactory receptors (Table 2, Supplementary Table 1). GPCR are cell membranes associated receptors that transduce extracellular signals into intracellular effector pathways and are activated by a large number of endogenous and exogenous ligands and stimuli (Busnelli et al., 2013; Kroeze et al., 2003; Lappano and Maggiolini, 2012; Perez, 2005). In our data signature, several genes were not only GPCR/olfactory genes but were also involved in other known mechanisms which may influence cancer development in the gastro-intestinal tract.

First, several genes were related to the activation of inflammation and chemokines. Ccl3 is a pro-inflammatory chemokine that modulates osteoclast differentiation by binding to GPCR (CCR1 and CCR5), and activates ERK and AKT signalling pathways (Vallet et al., 2011). It was regulated at day 2 and 14 in our data. Furthermore, Cxcl10 gene was modulated after 21 days of exposure to E171 which is in line with Krüger at al. who showed that *in vitro* exposure to TiO_2 NPs induced gene expression changes in inflammatory genes like Cxcl10 (Kruger et al., 2017). Moreover, Gpr75 activated by the chemokine Ccl5/Rantes (Liu et al., 2013) and Ptgdr2 has a role in the eosinophils migration and mediates the pro-inflammatory chemotaxis of eosinophils, basophils, and Th2 lymphocytes generated during allergic inflammation (Hirai et al., 2001; Monneret et al., 2001). These were both regulated after 2 days.

The second main known other function of these GPCR/olfactory and signalling genes is the activation of cancer related genes such as Ptch1 a tumour suppressor. Ghrhr is also involved in the growth of cancers such as breast and lung cancer (Barabutis et al., 2007). In our study, it was differentially expressed at 2, 7, and 14 days of exposure. Furthermore, cancer related DEG were also observed in signal transduction pathways at all time points. These DEG include fzd5 (frizzled homolog), Akt2, Ptch1 and Rous sarcoma oncogene (Src). Src, a member of the tyrosine kinase family, was up-regulated from 7 days of exposure. It has been shown that over-expression of this gene in colon cancer cells increases cell adhesion, invasion, and migration but not cell proliferation (Chung and Bunz, 2013; Playford and Schaller, 2004).

The effect of E171 on cancer related genes was observed from 7 days of exposure onwards. This effect might also have been induced indirectly via the immune system, as suggested by the activation of genes such as Trp53 (synonym of Tp53) and Pad. These are involved in regulating p53 and nuclear receptor target genes and play a role in the formation of NETs and antibacterial innate immunity (Table 6, in ref [Proquin et al., 2017b]) (Wang and Wang, 2013). After 14 days, cancer related genes and their related pathways were activated with 8 DEG involved in cell death upon oxidative stress and activation of cancer (Firat and Niedermann, 2016; Futreal et al., 2004; Ortega-Molina and Serrano, 2013; Playford and Schaller, 2004) (Table 7, in ref [Proquin et al., 2017b]). Over time, a total of 11 DEG have been identified that play a role in cancer and of which 7 are known to be specifically involved in CRC via various mechanisms such as the activation of cancer signalling or via the immune response (Supplementary Fig. 1). This can be observed by the upregulation of Src gene which activates the PI3K/Akt (observed after 14 days of exposure), MAPK (observed at 2 days), Stat3, IL-8, and VEGF pathways from 7 days onwards. Enhancement of intestinal epithelial cell proliferation and protection from apoptosis is associated with the downregulation of the P2rx7. These effects are linked to an increased production of TGFβ1 (Hofman et al., 2015). Related mechanisms such as survival of stem cells in the gut were activated by the upregulation from 7 days of Lgr4 and Flywch1. These genes cause overexpression of E-cadherin and both cell migration and defects that mimic the canonical Wnt loss-of-function (Muhammad et al., 2013). Another type of mechanism is induced by the mutation of Ptch1, its mutation in CRC induces a upregulation of the Hedgehog downstream gene Gli1 (Chung and Bunz, 2013). In our study, this gene was significantly up-regulated from 2 to 14 days. Other genes over time are associated with CRC such as Diaph1 which was up-regulated from 7 days. Lin et al. have shown a significant correlation between colon cancer metastasis and expression of Diaph1; it is not detectable in normal colon cells but significantly upregulated in colon cancer metastasis (Lin et al., 2014). Chd7 gene was significantly up-regulated from 2 to 14 days in our experiment. Its mutation is found in many subtypes of CRC (Kim et al., 2011; Tahara et al., 2014). Finally, a suggested biomarker for breast cancer and colorectal cancer, Dyx1c1 (Kim et al., 2009; Rosin et al., 2012) was activated at 2 days and downregulated at 7 and 14 days of exposure in our study.

Other genes showing over-expression after 7 days of exposure are involved in different type of cancers but not specifically in CRC like Ghrhr in breast and lung cancer (Barabutis et al., 2007), L1cam which

supports metastasis and plays a major role in the malignancy of human tumours (Kiefel et al., 2012), and Eno1 which is often overexpressed in various human cancers and has been shown to play a critical role in glycolysis and in oncogenesis (Zhan et al., 2015). Furthermore, DEG at multiple time points in cell cycle may have a direct and indirect impact on the development of cancer by several mechanisms. First mechanism is the inhibition cell death and growth cell arrest with the upregulation of growth arrest-specific 2 like 1 (Gas2l1) gene (Benetti et al., 2001). A second mechanism is the effect on several translation factors such as the Cyfip1. Its protein binds to the translation initiation factor eIF4E and mediates translational repression in mammalian cells and its upregulation affects general mRNA translation (De Rubeis et al., 2013; Napoli et al., 2008). This effect can be observed at day 7 and 14 (after GSEA) with in the modulation of mRNA processing pathway. Another affected translation factor is the Transcription elongation factor A protein-like 5 (Tceal5) gene. It regulates transcription from RNA polymerase II promoter and transcription. In our data, it was downregulated from 2 to 14 days of exposure. A third mechanism involves the induction of RNA methylation with the upregulation from 7 days of tRNA methyltransferase 1 (Trmt1) gene (Davarniya et al., 2015).

Genes involved in the immune system were also affected by the presence of E171. This might also have an impact on the development of cancer. After 2 and 7 days of exposure, we observed a significant down-regulation of Hspa genes that are known to be active in the inflammation of the intestinal mucosa (Scieglinska et al., 2011). At day 2 and 14, genes involved in the MHC class I & II presentation (H2-M9, H2-M11 and H2-Ea-ps), mice HLA genes, were up- and down-regulated. According to Pernot et al., a downregulation but not complete loss of MHC class I expression could contribute to an escape from NK-cell and T-cell mediated surveillance (Pernot et al., 2014). In addition, after 14 days, 2 genes involved in the activation of the complement were downregulated. Our data is in line with previous findings where a systemic disturbance of cellular immune function after ingestion of food-grade TiO_2 in rats was also measured (Bettini et al., 2017). In the rats' Peyer's Patches, a significant decreased frequency of immunoregulatory Tregs and $CD4^+CD25^+$ T helpers was observed after 7 and 100 days. Furthermore, an inhibition of the immune response (Duan et al., 2010) and a reduction in immune capacity by the down-regulation of genes involved in the activation of the complement (Cui et al., 2015) were observed in mice liver after ingestion of TiO_2 NPs.

Immune responses can also be mediated by the activation of serotonin receptor genes. At day 14 and 21, serotonin or 5-hydroxytryptamine (5-HT) genes were regulated (Tables 7 and 8, in ref [Proquin et al., 2017b]). These genes encode for a neurotransmitter and hormone that contributes to the regulation of various physiological functions by its actions in the central nervous system and in other organ systems (Gershon and Tack, 2007). Enterochromaffin cells in the gastrointestinal tract are the main producers of peripheral 5-HT, and form the main source of serotonin in the human body (Gershon and Tack, 2007; Shajib and Khan, 2015). Peripheral 5-HT is a potent immune modulator and affects various immune cells such as dendritic cells through its receptors and via the process of serotonylation (Idzko et al., 2004; Shajib and Khan, 2015). Alterations in 5-HT signalling have been associated with tumour progression in prostate as well as breast cancer (Dizeyi et al., 2004), regulation of genes involved in bone development (observed at 14 days) (Yano et al., 2015) and described in inflammatory conditions of the gut, such as inflammatory bowel disease (Gershon and Tack, 2007). Hence, the activation of serotonin receptors may lead to a chain reaction where immune related genes are modulated, as well as inflammation.

Oxidative stress related genes were also induced by E171 starting from 7 days of exposure with an upregulation of DEG such as Trp53, Cabin1 and Mapkapk3. Furthermore, Ucp2 and Ucp3 were upregulated at 14 and 21 days and are activated when oxidative stress occurs. Their uncoupling activities of the oxidative phosphorylation in the mitochondria can be stimulated by superoxide anions, limiting ROS production by the mitochondrial respiratory chain (Rial and Zardoya, 2009; Robbins and Zhao, 2011). Previous studies suggested that Ucp2

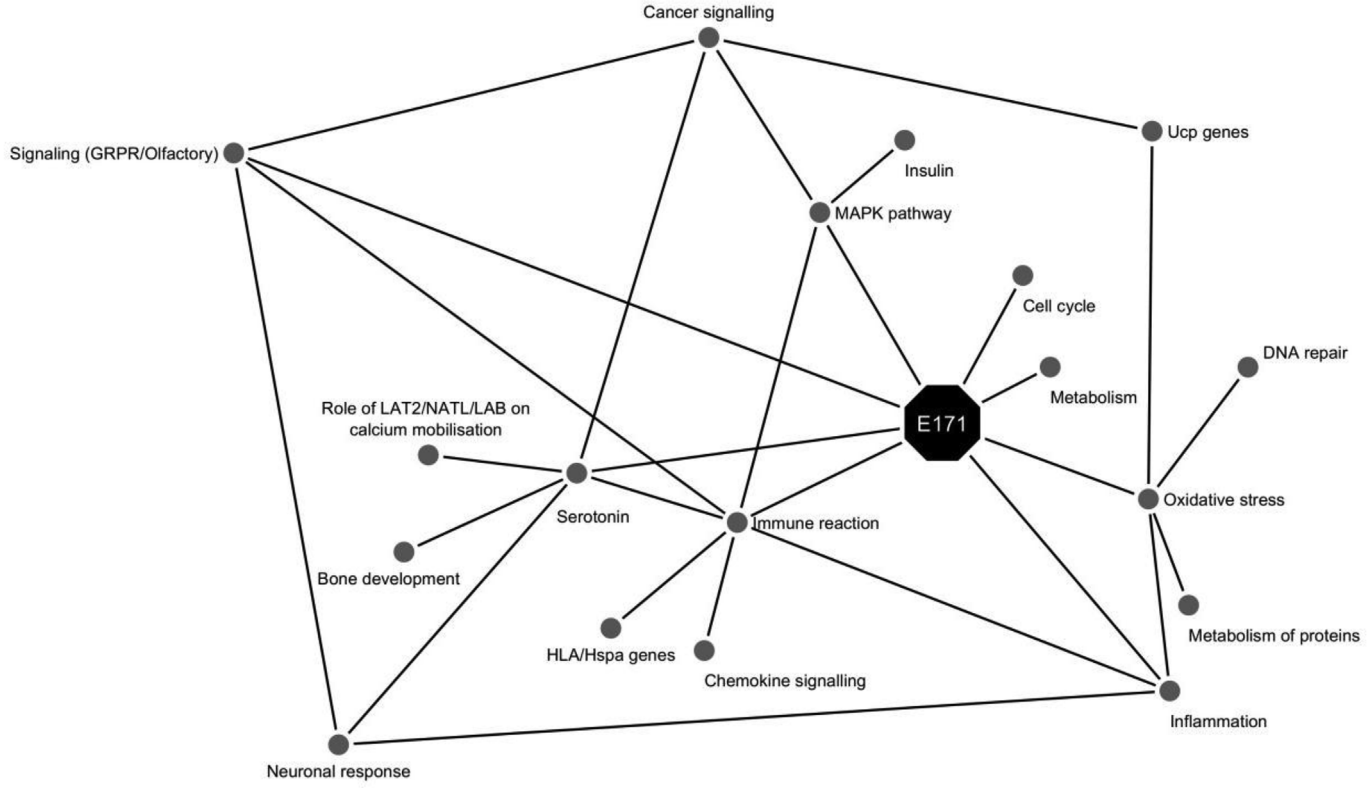

Fig. 5. Network created with Cytoscape to visualize the interaction between the different biological processes (circles) regulated after exposure to E171 (octagon) for 2, 7, 14, and 21 days.

may interact with oncogenes and tumour suppressor genes, providing a potential new mechanism of how Ucp2 contributes to cancer (Robbins and Zhao, 2011). These results showed that oxidative stress may be a constantly deregulated process over time and increases during prolonged exposure to E171. Possibly as a consequence of oxidative stress, pathways involved in DNA repair mechanisms were observed to be activated after 7 days of exposure. In total 7 pathways were identified after using the ORA method. All these pathways contain upregulated histone genes including which have a crucial role in transcription regulation, DNA repair, DNA replication, and chromosomal stability (Hunt et al., 2013; Rossetto et al., 2012). Furthermore, Cdkn1a/p21 is activated at 2, 14, and 21 days. It inhibits cell cycle progression and allows DNA repair to proceed while inhibiting apoptosis (Abbas and Dutta, 2009). This confirms previous finding where TiO_2 NPs was found to induce oxidative stress and DNA damage *in vitro* in different cell lines like HepG2 (from 0.1 μg/mL) or Caco-2 (from 10 or 20 μg/mL) (Gerloff et al., 2009; Proquin et al., 2017a; Shi et al., 2015) and also *in vivo* in other mouse models where oxidative stress as well as inflammation and DNA damage after intragastric administration was observed (Iavicoli et al., 2012; Trouiller et al., 2009; Wang et al., 2011). In addition to DNA repair, deregulation of the genes in the metabolism of proteins like post-translational protein modification indicate an effect of E171 towards development of cancer.

ROS production also induces changes in metabolic pathways. At 2 days, cellular stress regulates the mRNA stability of genes coding for heat shock proteins (Hsp) (Deka et al., 2016). Indeed, in the protein processing in endoplasmic reticulum pathway, 5 Hsp genes and 1 ubiquitin-conjugating enzyme gene were down-regulated. Furthermore, at day 7, after using the ORA method, insulin related signalling pathway genes were activated. A previous study reported an increase of plasma glucose in mice after exposure to TiO_2 via the activation of MAPK pathways by production of ROS (Hu et al., 2016). We also observed modulation of MAPK genes at 2 days of exposure causing a deregulation of MAPK signalling pathway (Table 2). At day 7 after ORA, the vitamin C metabolism pathway, contained genes such as glutathione S-transferase omega 2 (Gsto2) and 1 solute carrier family gene (Table 6, in ref [Proquin et al., 2017b]). Solute carrier genes were also observed after GSEA at day 7 with the SLC-mediated transmembrane transport pathway (Supplementary Table 1). Glutathione gene expression was downregulated which is in line with a previous study where they observed a significant reduction of cellular GSH content in human epidermal cells due to the radicals produced by the TiO_2 NPs (Shukla et al., 2011). Other genes such as genes involved in the synthesis of glycosylphosphatidylinositol (GPI) were also present in metabolism pathways and downregulated. These genes are involved in anchoring protein and glycoprotein to the cell surface in response to a stimuli (Swarts and Guo, 2012) and genes are activated with the presence of oxidative stress (Okada et al., 2014). One GPI genes Pigb was activated at day 2, 7, and 21 (Supplementary Fig. 1).

In order to conclude with respect to the effect of E171 over time, a network has been created in order to visualize the effect of exposure to E171 in the colon of mice (Fig. 5). This network shows that via different mechanisms, E171 activates the immune response, inflammation, GPCR/olfactory receptors, cell cycle, DNA repair, cancer related genes, metabolism and also serotonin receptors genes. This molecular response to the presence of E171 is very diverse and points towards an induction of inflammatory, immunological and specific cancer-related pathways in colon tissue that may explain the facilitated development of CRC by E171 reported previously (Urrutia-Ortega et al., 2016). The histopathological modifications observed at 14 and 21 days are resulting from these molecular changes.

4.1. Network analyses

Not all DEG could be related to molecular pathways by CPDB therefore a network analysis was performed with Genemania. This network analysis showed, after all genes known to be in pathways were extracted (after ORA), that the number of genes present in the pathway analysis was low (Fig. 3). This indicates that probably more genes, especially GPCR genes or olfactory genes, could be added in the corresponding pathways. At all investigated time points, the links by co-expression between the genes in molecular pathways and the centre of the network showed that the reaction after exposure to E171 in the colon was more extensive that what is actually known. Furthermore, most of the common genes between the different time points were contained in the centre of the network. The response of the colon cells to E171 was surely stronger than what can be observed by the current pathway classification. All the genes that could not directly be linked to pathways are of major interest for further studies since these might be related to yet unknown (biological) processes activated by exposure to E171.

5. Conclusion

In this study we observed gene expression changes in the distal colon of BALB/c mice after intragastric exposure to E171. We observed that E171 regulated GPCR/olfactory and serotonin gene receptors, induced oxidative stress and immune response pathways, activated genes for DNA repair and both up- and down-regulated genes involved in development of cancer, for instance colon cancer (Fig. 5). Furthermore, we identified responses to E171 on the expression of genes that thus far have not been defined as being involved in any pathway but may be functionally related to genes which have been assigned to biologically relevant pathways. Although no consistent effect of cell proliferation was observed, histology showed a hyperplastic epithelium in colonic crypts after 14 and 21 days of E171 ingestion. To the best of our knowledge this is the first time that a full genome analysis indicating biological effects induced by exposure to E171 in the colon of mice are described at the mRNA level. The results are in line with our previous study in which oxidative stress and DNA damage was observed *in vitro* in colon epithelial cells after E171 exposure (Proquin et al., 2017a) and could explain in part the facilitation by E171 of tumour growth in the colon of the BALB/c mouse model for CRC (Urrutia-Ortega et al., 2016). These results emphasize that the potentially harmful effects of E171 observed in the colon after oral exposure should be further investigated in order to guarantee the safe use of this food additive.

Conflict of interest

The authors declare that the research was conducted in the absence of any commercial or financial relationships that could be construed as a potential conflict of interest.

Acknowledgments

This work was supported in part by a grant from Maastricht University. Héloïse Proquin was enrolled in the PhD programme at Maastricht University. Additional support came from the Programa de Apoyo a los Profesores de Carrera (FESI-DIP-PAPCA-2016-11) para promover Grupos de Investigación and the Programa de Apoyos para la Superación del Personal Académico de la UNAM (comunicado no. 105/2016).

Appendix A. Supplementary data

Supplementary data related to this article can be found at http://dx.doi.org/10.1016/j.fct.2017.11.011

Transparency document

Transparency document related to this article can be found online at http://dx.doi.org/10.1016/j.fct.2017.11.011.

References

Abbas, T., Dutta, A., 2009. p21 in cancer: intricate networks and multiple activities. Nat. Rev. Cancer 9, 400–414.

Agilent, 2015. One-color Microarray-based Gene Expression Analysis. http://www.agilent.com/cs/library/usermanuals/Public/G4140-90040_GeneExpression_OneColor_6.9.pdf.

Alonso, R., Salavert, F., Garcia-Garcia, F., Carbonell-Caballero, J., Bleda, M., Garcia-Alonso, L., Sanchis-Juan, A., Perez-Gil, D., Marin-Garcia, P., Sanchez, R., Cubuk, C., Hidalgo, M.R., Amadoz, A., Hernansaiz-Ballesteros, R.D., Aleman, A., Tarraga, J., Montaner, D., Medina, I., Dopazo, J., 2015. Babelomics 5.0: functional interpretation for new generations of genomic data. Nucleic Acids Res. 43, W117–W121.

Barabutis, N., Tsellou, E., Schally, A.V., Kouloheri, S., Kalofoutis, A., Kiaris, H., 2007. Stimulation of proliferation of MCF-7 breast cancer cells by a transfected splice variant of growth hormone-releasing hormone receptor. Proc. Natl. Acad. Sci. U. S. A. 104, 5575–5579.

Benetti, R., Del Sal, G., Monte, M., Paroni, G., Brancolini, C., Schneider, C., 2001. The death substrate Gas2 binds m-calpain and increases susceptibility to p53-dependent apoptosis. EMBO J. 20, 2702–2714.

Bettini, S., Boutet-Robinet, E., Cartier, C., Comera, C., Gaultier, E., Dupuy, J., Naud, N., Tache, S., Grysan, P., Reguer, S., Thieriet, N., Refregiers, M., Thiaudiere, D., Cravedi, J.P., Carriere, M., Audinot, J.N., Pierre, F.H., Guzylack-Piriou, L., Houdeau, E., 2017. Food-grade TiO2 impairs intestinal and systemic immune homeostasis, initiates preneoplastic lesions and promotes aberrant crypt development in the rat colon. Sci. Rep. 7, 40373.

Busnelli, M., Mauri, M., Parenti, M., Chini, B., 2013. Analysis of GPCR dimerization using acceptor photobleaching resonance energy transfer techniques. Methods Enzymol. 521, 311–327.

Castro, N.P., Osorio, C.A., Torres, C., Bastos, E.P., Mourao-Neto, M., Soares, F.A., Brentani, H.P., Carraro, D.M., 2008. Evidence that molecular changes in cells occur before morphological alterations during the progression of breast ductal carcinoma. Breast Cancer Res. 10, R87.

Chen, Z., Wang, Y., Ba, T., Li, Y., Pu, J., Chen, T., Song, Y., Gu, Y., Qian, Q., Yang, J., Jia, G., 2014. Genotoxic evaluation of titanium dioxide nanoparticles in vivo and in vitro. Toxicol. Lett. 226, 314–319.

Chung, J.H., Bunz, F., 2013. A loss-of-function mutation in PTCH1 suggests a role for autocrine hedgehog signaling in colorectal tumorigenesis. Oncotarget 4, 2208–2211.

Cline, M.S., Smoot, M., Cerami, E., Kuchinsky, A., Landys, N., Workman, C., Christmas, R., Avila-Campilo, I., Creech, M., Gross, B., Hanspers, K., Isserlin, R., Kelley, R., Killcoyne, S., Lotia, S., Maere, S., Morris, J., Ono, K., Pavlovic, V., Pico, A.R., Vailaya, A., Wang, P.L., Adler, A., Conklin, B.R., Hood, L., Kuiper, M., Sander, C., Schmulevich, I., Schwikowski, B., Warner, G.J., Ideker, T., Bader, G.D., 2007. Integration of biological networks and gene expression data using Cytoscape. Nat. Protoc. 2, 2366–2382.

Cui, Y., Gong, X., Duan, Y., Li, N., Hu, R., Liu, H., Hong, M., Zhou, M., Wang, L., Wang, H., Hong, F., 2010. Hepatocyte apoptosis and its molecular mechanisms in mice caused by titanium dioxide nanoparticles. J. Hazard Mater 183, 874–880.

Cui, Y., Liu, H., Ze, Y., Zhang, Z., Hu, Y., Cheng, Z., Cheng, J., Hu, R., Gao, G., Wang, L., Tang, M., Hong, F., 2015. Corrigendum: gene expression in liver injury caused by long-term exposure to titanium dioxide nanoparticles in mice. Toxicol. Sci. 146, 202.

Davarniya, B., Hu, H., Kahrizi, K., Musante, L., Fattahi, Z., Hosseini, M., Maqsoud, F., Farajollahi, R., Wienker, T.F., Ropers, H.H., Najmabadi, H., 2015. The role of a novel TRMT1 gene mutation and rare GRM1 gene defect in intellectual disability in two azeri families. PLoS One 10, e0129631.

de Kok, T.M., de Waard, P., Wilms, L.C., van Breda, S.G., 2010. Antioxidative and anti-genotoxic properties of vegetables and dietary phytochemicals: the value of genomics biomarkers in molecular epidemiology. Mol. Nutr. Food Res. 54, 208–217.

De Rubeis, S., Pasciuto, E., Li, K.W., Fernandez, E., Di Marino, D., Buzzi, A., Ostroff, L.E., Klann, E., Zwartkruis, F.J., Komiyama, N.H., Grant, S.G., Poujol, C., Choquet, D., Achsel, T., Posthuma, D., Smit, A.B., Bagni, C., 2013. CYFIP1 coordinates mRNA translation and cytoskeleton remodeling to ensure proper dendritic spine formation. Neuron 79, 1169–1182.

Deka, K., Singh, A., Chakraborty, S., Mukhopadhyay, R., Saha, S., 2016. Protein arginylation regulates cellular stress response by stabilizing HSP70 and HSP40 transcripts. Cell Death Discov. 2, 16074.

Dizeyi, N., Bjartell, A., Nilsson, E., Hansson, J., Gadaleanu, V., Cross, N., Abrahamsson, P.A., 2004. Expression of serotonin receptors and role of serotonin in human prostate cancer tissue and cell lines. Prostate 59, 328–336.

Dorier, M., Beal, D., Marie-Desvergne, C., Dubosson, M., Barreau, F., Houdeau, E., Herlin-Boime, N., Carriere, M., 2017. Continuous in vitro exposure of intestinal epithelial cells to E171 food additive causes oxidative stress, inducing oxidation of DNA bases but no endoplasmic reticulum stress. Nanotoxicology 1–54.

Duan, Y., Liu, J., Ma, L., Li, N., Liu, H., Wang, J., Zheng, L., Liu, C., Wang, X., Zhao, X., Yan, J., Wang, S., Wang, H., Zhang, X., Hong, F., 2010. Toxicological characteristics of nanoparticulate anatase titanium dioxide in mice. Biomaterials 31, 894–899.

Dudefoi, W., Moniz, K., Allen-Vercoe, E., Ropers, M.H., Walker, V.K., 2017. Impact of food grade and nano-TiO2 particles on a human intestinal community. Food Chem. Toxicol. 106, 242–249.

EFSA, 2016. Re-evaluation of titanium dioxide (E 171) as a food additive. EFSA J. 14 e04545-n/a.

Espin-Perez, A., de Kok, T.M., Jennen, D.G., Hendrickx, D.M., De Coster, S., Schoeters, G., Baeyens, W., van Larebeke, N., Kleinjans, J.C., 2015. Distinct genotype-dependent differences in transcriptome responses in humans exposed to environmental carcinogens. Carcinogenesis 36, 1154–1161.

EU, 2012. Regulation No 231-2012 on food additives. Official J. Eur. Union 83, 1–295.

Firat, E., Niedermann, G., 2016 Aug 23. FoxO proteins or loss of functional p53 maintain stemness of glioblastoma stem cells and survival after ionizing radiation plus PI3K/mTOR inhibition. Oncotarget 7 (34), 54883–54896. http://dx.doi.org/10.18632/oncotarget.10702.

Futreal, P.A., Coin, L., Marshall, M., Down, T., Hubbard, T., Wooster, R., Rahman, N., Stratton, M.R., 2004. A census of human cancer genes. Nat. Rev. Cancer 4, 177–183.

Gadbury, G.L., Page, G.P., Edwards, J., Kayo, T., Prolla, T.A., Weindruch, R., Permana, P.A., Mountz, J.D., Allison, D.B., 2004. Power and sample size estimation in high dimensional biology. Stat. Methods Med. Res. 13, 325–338.

Gerloff, K., Albrecht, C., Boots, A.W., Forster, I., Schins, R.P.F., 2009. Cytotoxicity and oxidative DNA damage by nanoparticles in human intestinal Caco-2 cells. Nanotoxicology 3, 355–364.

Gershon, M.D., Tack, J., 2007. The serotonin signaling system: from basic understanding to drug development for functional GI disorders. Gastroenterology 132, 397–414.

Globocan, 2012. Cancer Fact Sheets: Colorectal Cancer.

Haggar, F.A., Boushey, R.P., 2009. Colorectal cancer epidemiology: incidence, mortality, survival, and risk factors. Clin. Colon Rectal Surg. 22, 191–197.

Herwig, R., Hardt, C., Lienhard, M., Kamburov, A., 2016. Analyzing and interpreting genome data at the network level with ConsensusPathDB. Nat. Protoc. 11, 1889–1907.

Hirai, H., Tanaka, K., Yoshie, O., Ogawa, K., Kenmotsu, K., Takamori, Y., Ichimasa, M., Sugamura, K., Nakamura, M., Takano, S., Nagata, K., 2001. Prostaglandin D2 selectively induces chemotaxis in T helper type 2 cells, eosinophils, and basophils via seven-transmembrane receptor CRTH2. J. Exp. Med. 193, 255–261.

Hofman, P., Cherfils-Vicini, J., Bazin, M., Ilie, M., Juhel, T., Hebuterne, X., Gilson, E., Schmid-Alliana, A., Boyer, O., Adriouch, S., Vouret-Craviari, V., 2015. Genetic and pharmacological inactivation of the purinergic P2RX7 receptor dampens inflammation but increases tumor incidence in a mouse model of colitis-associated cancer. Cancer Res. 75, 835–845.

Hu, H., Li, L., Guo, Q., Jin, S., Zhou, Y., Oh, Y., Feng, Y., Wu, Q., Gu, N., 2016. A mechanistic study to increase understanding of titanium dioxide nanoparticles-increased plasma glucose in mice. Food Chem. Toxicol. 95, 175–187.

Hunt, C.R., Ramnarain, D., Horikoshi, N., Iyengar, P., Pandita, R.K., Shay, J.W., Pandita, T.K., 2013. Histone modifications and DNA double-strand break repair after exposure to ionizing radiations. Radiat. Res. 179, 383–392.

IARC, 2010. IARC monographs on the evaluation of carcinogenic risks to humans: carbon black. Titanium Dioxide Talc 93.

Iavicoli, I., Leso, V., Bergamaschi, A., 2012. Toxicological effects of titanium dioxide nanoparticles: a review of in vivo studies. J. Nanomater. 2012http://dx.doi.org/10.1155/2012/964381. Article ID 964381, 36 pages.

Idzko, M., Panther, E., Stratz, C., Muller, T., Bayer, H., Zissel, G., Durk, T., Sorichter, S., Di Virgilio, F., Geissler, M., Fiebich, B., Herouy, Y., Elsner, P., Norgauer, J., Ferrari, D., 2004. The serotoninergic receptors of human dendritic cells: identification and coupling to cytokine release. J. Immunol. 172, 6011–6019.

Jin, C.Y., Zhu, B.S., Wang, X.F., Lu, Q.H., 2008. Cytotoxicity of titanium dioxide nanoparticles in mouse fibroblast cells. Chem. Res. Toxicol. 21, 1871–1877.

Kamburov, A., Stelzl, U., Lehrach, H., Herwig, R., 2013. The ConsensusPathDB interaction database: 2013 update. Nucleic Acids Res. 41, D793–D800.

Kiefel, H., Bondong, S., Hazin, J., Ridinger, J., Schirmer, U., Riedle, S., Altevogt, P., 2012. L1CAM: a major driver for tumor cell invasion and motility. Cell Adh Migr. 6, 374–384.

Kim, M.S., Chung, N.G., Kang, M.R., Yoo, N.J., Lee, S.H., 2011. Genetic and expressional alterations of CHD genes in gastric and colorectal cancers. Histopathology 58, 660–668.

Kim, Y.J., Huh, J.W., Kim, D.S., Bae, M.I., Lee, J.R., Ha, H.S., Ahn, K., Kim, T.O., Song, G.A., Kim, H.S., 2009. Molecular characterization of the DYX1C1 gene and its application as a cancer biomarker. J. Cancer Res. Clin. Oncol. 135, 265–270.

Kroeze, W.K., Sheffler, D.J., Roth, B.L., 2003. G-protein-coupled receptors at a glance. J. Cell Sci. 116, 4867–4869.

Kruger, K., Schrader, K., Klempt, M., 2017. Cellular response to titanium dioxide nanoparticles in intestinal epithelial Caco-2 cells is dependent on endocytosis-associated structures and mediated by EGFR. Nanomater. (Basel) 7.

Lappano, R., Maggiolini, M., 2012. GPCRs and cancer. Acta Pharmacol. Sin. 33, 351–362.

Lin, Y.N., Izbicki, J.R., Konig, A., Habermann, J.K., Blechner, C., Lange, T., Schumacher, U., Windhorst, S., 2014. Expression of DIAPH1 is up-regulated in colorectal cancer and its down-regulation strongly reduces the metastatic capacity of colon carcinoma cells. International journal of cancer. J. Int. du cancer 134, 1571–1582.

Liu, B., Hassan, Z., Amisten, S., King, A.J., Bowe, J.E., Huang, G.C., Jones, P.M., Persaud, S.J., 2013. The novel chemokine receptor, G-protein-coupled receptor 75, is expressed by islets and is coupled to stimulation of insulin secretion and improved glucose homeostasis. Diabetologia 56, 2467–2476.

Liu, R., Yin, L.H., Pu, Y.P., Li, Y.H., Zhang, X.Q., Liang, G.Y., Li, X.B., Zhang, J., Li, Y.F., Zhang, X.Y., 2010. The immune toxicity of titanium dioxide on primary pulmonary alveolar macrophages relies on their surface area and crystal structure. J. Nanosci. Nanotechnol. 10, 8491–8499.

Macwan, D.P., Dave, P.N., Chaturvedi, S., 2011. A review on nano-TiO2 sol-gel type syntheses and its applications. J. Mater Sci. 46, 3669–3686.

Monneret, G., Gravel, S., Diamond, M., Rokach, J., Powell, W.S., 2001. Prostaglandin D-2 is a potent chemoattractant for human eosinophils that acts via a novel DP receptor. Blood 98, 1942–1948.

Montojo, J., Zuberi, K., Rodriguez, H., Kazi, F., Wright, G., Donaldson, S.L., Morris, Q., Bader, G.D., 2010. GeneMANIA Cytoscape plugin: fast gene function predictions on the desktop. Bioinformatics 26, 2927–2928.

Mostafavi, S., Ray, D., Warde-Farley, D., Grouios, C., Morris, Q., 2008. GeneMANIA: a real-time multiple association network integration algorithm for predicting gene function. Genome Biol. 9 (Suppl. 1), S4.

Muhammad, B., Saadeddin, A., Spencer, B., Ibrahim, E.-S., Ilyas, M., Nater, A., 2013. Identification, Characterisation and Functional Analyses of Novel Beta-catenin Associated Protein, FLYWCH1. PhD thesis. University of Nottingham.
Napoli, I., Mercaldo, V., Boyl, P.P., Eleuteri, B., Zalfa, F., De Rubeis, S., Di Marino, D., Mohr, E., Massimi, M., Falconi, M., Witke, W., Costa-Mattioli, M., Sonenberg, N., Achsel, T., Bagni, C., 2008. The fragile X syndrome protein represses activity-dependent translation through CYFIP1, a new 4E-BP. Cell 134, 1042–1054.
Okada, N., Ogawa, J., Shima, J., 2014. Comprehensive analysis of genes involved in the oxidative stress tolerance using yeast heterozygous deletion collection. Fems Yeast Res. 14, 425–434.
Ortega-Molina, A., Serrano, M., 2013. PTEN in cancer, metabolism, and aging. Trends Endocrinol. Metab. 24, 184–189.
Page, G.P., Edwards, J.W., Gadbury, G.L., Yelisetti, P., Wang, J., Trivedi, P., Allison, D.B., 2006. The PowerAtlas: a power and sample size atlas for microarray experimental design and research. Bmc Bioinforma. 7, 84.
Park, E.J., Yi, J., Chung, K.H., Ryu, D.Y., Choi, J., Park, K., 2008. Oxidative stress and apoptosis induced by titanium dioxide nanoparticles in cultured BEAS-2B cells. Toxicol. Lett. 180, 222–229.
Perez, D.M., 2005. From plants to man: the GPCR “tree of life”. Mol. Pharmacol. 67, 1383–1384.
Pernot, S., Terme, M., Voron, T., Colussi, O., Marcheteau, E., Tartour, E., Taieb, J., 2014. Colorectal cancer and immunity: what we know and perspectives. World J. Gastroentero 20, 3738–3750.
Peters, R.J., van Bemmel, G., Herrera-Rivera, Z., Helsper, H.P., Marvin, H.J., Weigel, S., Tromp, P.C., Oomen, A.G., Rietveld, A.G., Bouwmeester, H., 2014. Characterization of titanium dioxide nanoparticles in food products: analytical methods to define nanoparticles. J. Agric. Food Chem. 62, 6285–6293.
Playford, M.P., Schaller, M.D., 2004. The interplay between Src and integrins in normal and tumor biology. Oncogene 23, 7928–7946.
Proquin, H., Rodriguez-Ibarra, C., Moonen, C.G., Urrutia Ortega, I.M., Briede, J.J., de Kok, T.M., van Loveren, H., Chirino, Y.I., 2017 Jana. Titanium dioxide food additive (E171) induces ROS formation and genotoxicity: contribution of micro and nano-sized fractions. Mutagenesis 32 (1), 139–149. http://dx.doi.org/10.1093/mutage/gew051. Epub 2016 Oct 27.
Proquin, H., Jetten, M.J., Jonkhout, M.C.M., Garduño-Balderas, L.G., Briedé, J.J., de Kok, T.M., Chirino, Y.I., van Loveren, H., 2017b. Gene Expression Changes After Time Course Exposure to Food-grade E171 in Colon of Mice. Data in Brief, Submitted.
Qiagen, 2012. RNeasy Mini Handbook. https://www.qiagen.com/us/resources/resourcedetail?id=14e7cf6e-521a-4cf7-8cbc-bf9f6fa33e24&lang=en.
Reeves, J.F., Davies, S.J., Dodd, N.J., Jha, A.N., 2008. Hydroxyl radicals (*OH) are associated with titanium dioxide (TiO(2)) nanoparticle-induced cytotoxicity and oxidative DNA damage in fish cells. Mutat. Res. 640, 113–122.
Reich, M., Liefeld, T., Gould, J., Lerner, J., Tamayo, P., Mesirov, J.P., 2006. GenePattern 2.0. Nat. Genet. 38, 500–501.
Rial, E., Zardoya, R., 2009. Oxidative stress, thermogenesis and evolution of uncoupling proteins. J. Biol. 8, 58.
Robbins, D., Zhao, Y., 2011. New aspects of mitochondrial Uncoupling Proteins (UCPs) and their roles in tumorigenesis. Int. J. Mol. Sci. 12, 5285–5293.
Rompelberg, C., Heringa, M.B., van Donkersgoed, G., Drijvers, J., Roos, A., Westenbrink, S., Peters, R., van Bemmel, G., Brand, W., Oomen, A.G., 2016. Oral intake of added titanium dioxide and its nanofraction from food products, food supplements and toothpaste by the Dutch population. Nanotoxicology 10, 1404–1414.
Rosin, G., Hannelius, U., Lindstrom, L., Hall, P., Bergh, J., Hartman, J., Kere, J., 2012. The dyslexia candidate gene DYX1C1 is a potential marker of poor survival in breast cancer. BMC Cancer 12, 79.
Rossetto, D., Avvakumov, N., Cote, J., 2012. Histone phosphorylation: a chromatin modification involved in diverse nuclear events. Epigenetics 7, 1098–1108.
Scieglinska, D., Piglowski, W., Chekan, M., Mazurek, A., Krawczyk, Z., 2011. Differential expression of HSPA1 and HSPA2 proteins in human tissues; tissue microarray-based immunohistochemical study. Histochem Cell Biol. 135, 337–350.
Shajib, M.S., Khan, W.I., 2015. The role of serotonin and its receptors in activation of immune responses and inflammation. Acta Physiol. (Oxf) 213, 561–574.
Shi, Z.Q., Niu, Y.J., Wang, Q., Shi, L., Guo, H.C., Liu, Y., Zhu, Y., Liu, S.F., Liu, C., Chen, X., Zhang, R., 2015. Reduction of DNA damage induced by titanium dioxide nanoparticles through Nrf2 in vitro and in vivo. J. Hazard. Mater. 298, 310–319.
Shukla, R.K., Sharma, V., Pandey, A.K., Singh, S., Sultana, S., Dhawan, A., 2011. ROS-mediated genotoxicity induced by titanium dioxide nanoparticles in human epidermal cells. Toxicol In Vitro 25, 231–241.
Smyth, G., 2017. Linear Models for Microarray Data. https://www.bioconductor.org/packages/devel/bioc/manuals/limma/man/limma.pdf.
Smyth, G.K., 2005. Limma: Linear Models for Microarray Data, Bioinformatics and Computational Biology Solutions Using R and Bioconductor. Springer, pp. 397–420.
Swarts, B.M., Guo, Z., 2012. Chemical synthesis of glycosylphosphatidylinositol anchors. Adv. Carbohydr. Chem. Biochem. 67, 137–219.
Tahara, T., Yamamoto, E., Madireddi, P., Suzuki, H., Maruyama, R., Chung, W., Garriga, J., Jelinek, J., Yamano, H.O., Sugai, T., Kondo, Y., Toyota, M., Issa, J.P., Estecio, M.R., 2014. Colorectal carcinomas with CpG island methylator phenotype 1 frequently contain mutations in chromatin regulators. Gastroenterology 146, 530–538 e535.
Trouiller, B., Reliene, R., Westbrook, A., Solaimani, P., Schiestl, R.H., 2009. Titanium dioxide nanoparticles induce DNA damage and genetic instability in vivo in mice. Cancer Res. 69, 8784–8789.
Urrutia-Ortega, I.M., Garduno-Balderas, L.G., Delgado-Buenrostro, N.L., Freyre-Fonseca, V., Flores-Flores, J.O., Gonzalez-Robles, A., Pedraza-Chaverri, J., Hernandez-Pando, R., Rodriguez-Sosa, M., Leon-Cabrera, S., Terrazas, L.I., van Loveren, H., Chirino, Y.I., 2016. Food-grade titanium dioxide exposure exacerbates tumor formation in colitis associated cancer model. Food Chem. Toxicol. 93, 20–31.
Vallet, S., Pozzi, S., Patel, K., Vaghela, N., Fulciniti, M.T., Veiby, P., Hideshima, T., Santo, L., Cirstea, D., Scadden, D.T., Anderson, K.C., Raje, N., 2011. A novel role for CCL3 (MIP-1alpha) in myeloma-induced bone disease via osteocalcin downregulation and inhibition of osteoblast function. Leukemia 25, 1174–1181.
Wang, J., Li, N., Zheng, L., Wang, S., Wang, Y., Zhao, X., Duan, Y., Cui, Y., Zhou, M., Cai, J., Gong, S., Wang, H., Hong, F., 2011. P38-Nrf-2 signaling pathway of oxidative stress in mice caused by nanoparticulate TiO2. Biol. Trace Elem. Res. 140, 186–197.
Wang, S., Wang, Y., 2013. Peptidylarginine deiminases in citrullination, gene regulation, health and pathogenesis. Biochim. Biophys. Acta 1829, 1126–1135.
Waters, M.D., Fostel, J.M., 2004. Toxicogenomics and systems toxicology: aims and prospects. Nat. Rev. Genet. 5, 936–948.
Weir, A., Westerhoff, P., Fabricius, L., Hristovski, K., von Goetz, N., 2012. Titanium dioxide nanoparticles in food and personal care products. Environ. Sci. Technol. 46, 2242–2250.
Yano, J.M., Yu, K., Donaldson, G.P., Shastri, G.G., Ann, P., Ma, L., Nagler, C.R., Ismagilov, R.F., Mazmanian, S.K., Hsiao, E.Y., 2015. Indigenous bacteria from the gut microbiota regulate host serotonin biosynthesis. Cell 161, 264–276.
Zhan, P., Wang, Y., Zhao, S., Liu, C., Wang, Y., Wen, M., Mao, J.H., Wei, G., Zhang, P., 2015. FBXW7 negatively regulates ENO1 expression and function in colorectal cancer. Lab. Invest 95, 995–1004.
Zijno, A., De Angelis, I., De Berardis, B., Andreoli, C., Russo, M.T., Pietraforte, D., Scorza, G., Degan, P., Ponti, J., Rossi, F., Barone, F., 2015. Different mechanisms are involved in oxidative DNA damage and genotoxicity induction by ZnO and TiO nanoparticles in human colon carcinoma cells. Toxicol In Vitro 29, 1503–1512.